doi:10.1093/brain/awr021 Brain 2011: 134; 1199–1210 | 1199

BRAIN
A JOURNAL OF NEUROLOGY

Motor pathway injury in patients with periventricular leucomalacia and spastic diplegia

Jong Doo Lee,[1,2,3,*] Hae-Jeong Park,[1,2,3,*] Eun Sook Park,[4,*] Maeng-Keun Oh,[1] Bumhee Park,[1,3] Dong-Wook Rha,[4] Sung-Rae Cho,[4] Eung Yeop Kim,[1,2] Jun Young Park,[1] Chul Hoon Kim,[5] Dong Goo Kim[5] and Chang Il Park[4]

1 Department of Diagnostic Radiology, Division of Nuclear Medicine, Yonsei University College of Medicine, Seoul, Korea
2 Research Institute of Radiological Science, Yonsei University College of Medicine, Seoul, Korea
3 Brain Korea 21 Project for Medical Science, Yonsei University College of Medicine, Seoul, Korea
4 Department of Rehabilitation Medicine, Yonsei University College of Medicine, Seoul, Korea
5 Department of Pharmacology, Yonsei University College of Medicine, Seoul, Korea

*These authors contributed equally to this work.

Correspondence to: Jong Doo Lee, MD, PhD,
Professor of Diagnostic Radiology,
Director of Nuclear Medicine,
Yonsei University,
College of Medicine,
250 Seongsan-ro,
Seodaemun-gu,
Seoul, 120-752,
Korea
E-mail: jdlee@yuhs.ac

Periventricular leucomalacia has long been investigated as a leading cause of motor and cognitive dysfunction in patients with spastic diplegic cerebral palsy. However, patients with periventricular leucomalacia on conventional magnetic resonance imaging do not always have motor dysfunction and preterm children without neurological abnormalities may have periventricular leucomalacia. In addition, it is uncertain whether descending motor tract or overlying cortical injury is related to motor impairment. To investigate the relationship between motor pathway injury and motor impairment, we conducted voxelwise correlation analysis using tract-based spatial statistics of white matter diffusion anisotropy and voxel-based-morphometry of grey matter injury in patients with periventricular leucomalacia and spastic diplegia ($n = 43$, mean 12.86 ± 4.79 years, median 12 years). We also evaluated motor cortical and thalamocortical connectivity at resting state in 11 patients using functional magnetic resonance imaging. The functional connectivity results of patients with spastic diplegic cerebral palsy were compared with those of age-matched normal controls. Since γ-aminobutyric acid$_A$ receptors play an important role in the remodelling process, we measured neuronal γ-aminobutyric acid$_A$ receptor binding potential with dynamic positron emission tomography scans ($n = 27$) and compared the binding potential map of the patient group with controls ($n = 20$). In the current study, white matter volume reduction did not show significant correlation with motor dysfunction. Although fractional anisotropy within most of the major white matter tracts were significantly lower than that of age-matched healthy controls ($P < 0.05$, family wise error corrected), fractional anisotropy mainly within the bilateral corticospinal tracts and posterior body and isthmus of the corpus callosum showed more significant correlation with motor dysfunction ($P < 0.03$) than thalamocortical pathways ($P < 0.05$, family-wise error corrected). Cortical volume of the pre- and post-central gyri and the paracentral lobule tended to be negatively correlated with motor function. The motor cortical connectivity was diminished mainly within the bilateral

Received August 4, 2010. Revised November 23, 2010. Accepted December 12, 2010. Advance Access publication March 7, 2011

somatosensory cortex, paracentral lobule, cingulate motor area and visual cortex in the patient group. Thalamovisual connectivity was not diminished despite severe optic radiation injury. γ-aminobutyric acid$_A$ receptor binding potential was focally increased within the lower extremity homunculus, cingulate cortex, visual cortex and cerebellum in the patient group ($P < 0.05$, false discovery rate corrected). In conclusion, descending motor tract injury along with overlying cortical volume reduction and reduced functional connectivity appears to be a leading pathophysiological mechanism of motor dysfunction in patients with periventricular leucomalacia. Increased regional γ-aminobutyric acid$_A$ receptor binding potential appears to result from a compensatory plasticity response after prenatal brain injury.

Keywords: corticospinal tract; functional connectivity; motor dysfunction; periventricular leucomalacia; tract-based spatial statistics
Abbreviations: BA = Brodmann area; GABA = γ-aminobutyric acid; GMFCS = gross motor function classification system

Introduction

Periventricular leucomalacia has long been investigated as a leading cause of motor and cognitive impairment in subjects who were born prematurely with a low birth weight or very low birth weight. The main neuropathological feature is a focal or diffuse necrosis of cerebral white matter with loss of all cellular elements. Although necrosis can be macroscopic in size and readily seen on MRI or ultrasonography as a cystic lesion (cystic periventricular leucomalacia), it is observed in <5% of infants with very low birth weight. More commonly, microscopic necrosis with glial scars is diffusely involved in cerebral white matter (diffuse periventricular leucomalacia). Although cystic periventricular leucomalacia is more correlated with motor impairment, the diffuse type of periventricular leucomalacia accounts for the vast majority of periventricular leucomalacia cases (Volpe *et al.*, 2009), and it is known to be a high risk factor of spastic diplegic cerebral palsy. Conventional brain MRI study can be used in the detection of structural abnormalities, and it provides information on the timing and extent of the hypoxic-ischaemic insult in patients with cerebral palsy (Bax *et al*., 2006). Previous MRI studies in adolescents born with prematurity and very low birth weight demonstrated high incidence of structural abnormalities that are compatible with periventricular leucomalacia such as dilatation of the occipital horn of lateral ventricles, periventricular white matter volume reduction or thinning of corpus callosum. Among them, ~10% had spastic diplegia symptoms (Vangberg *et al*., 2006; Skranes *et al*., 2007). In contrast, white matter injury cannot be seen in up to 29% of patients with spastic diplegic cerebral palsy on conventional MRI (Bax *et al*., 2006). A recent study reported that the incidence of cerebral palsy was 24% in moderate periventricular leucomalacia and 67% in severe periventricular leucomalacia cases (Woodward *et al*., 2006). Therefore, the severity of white matter injury shown on conventional MRI does not appear to be closely correlated with the severity of motor impairment.

Currently, diffusion tensor imaging is widely used for the evaluation of the white matter tract injury in various brain diseases since diffusion tensor imaging is more sensitive than conventional MRI in the detection of microstructural damage. Previous data demonstrated white matter injury on diffusion tensor imaging while conventional MRI failed to demonstrate any structural abnormality in preterm infants (Arzoumanian *et al*., 2003; Anjari *et al*., 2007). Nevertheless, until recently there has been a lack of voxelwise cross-correlation study between motor pathway injury and motor dysfunction. In this study, we assessed the correlation, on a voxelwise basis, between fractional anisotropy values of the major white matter tracts and the severity of motor dysfunction using tract-based spatial statistics. Our primary purpose was to investigate whether descending motor tract injury is closely correlated with motor dysfunction in patients with periventricular leucomalacia.

Grey matter injury is also commonly associated with periventricular leucomalacia (Inder *et al*., 1999, 2005; Pierson *et al*., 2007). However, it remains to be further elucidated whether regional grey matter injury is involved in the pathogenesis of motor dysfunction in patients with periventricular leucomalacia. Therefore, we also performed correlation analysis between motor dysfunction scale and regional grey matter integrity such as regional cortical volume reduction and alterations in motor cortical or thalamocortical functional connectivity. We evaluated regional γ-aminobutyric acid (GABA$_A$) receptor binding potential in patients with spastic diplegic cerebral palsy and compared the results with those of healthy controls, which could provide valuable information regarding to brain reorganization process after prenatal hypoxic-ischaemic insult since GABAergic neural transmission plays an important role in the repair process of the glutamatergic system (Schwartz-Bloom and Sah, 2001).

Materials and methods

Subjects

In total, 43 children or adults (26 males and 17 females, age range 6–29 years, mean age 12.98 ± 5.26 years, median 12 years) with spastic diplegia symptoms and diffuse periventricular white matter injury on conventional MRI were included. Subjects with structural abnormalities such as a cortical infarction, malformation or any other type of congenital anomalies in the cortical and subcortical grey matter regions on MRI were not included in the current study. All spastic diplegic cerebral palsy subjects were born prematurely (<37 weeks, range 26–34 weeks, mean 30.91 ± 2.10, median 32 weeks) with a low birth weight ($n = 32$), very low birth weight ($n = 9$) or extremely low birth weight ($n = 2$) (range 0.93–2.48 kg, mean 1.69 ± 0.36 kg) but born appropriate for gestational age. Three subjects were born from a twin pregnancy. Twelve subjects had history of perinatal asphyxia, however, grey matter injury such as parasagittal ulegyria

or cortical infarction that might produce permanent motor dysfunction was not observed on conventional MRI. Other risk factors for periventricular leucomalacia such as chronic lung diseases, intrauterine infection or prolonged rupture of membranes were not evident in their medical records. Three subjects had eye problems such as strabismus ($n = 2$) or decreased visual function ($n = 1$), five subjects had speech problems and three subjects had neurocognitive delay. All patients received orthopaedic surgery, such as heel cord lengthening to reduce spasticity symptoms, 3–58 months prior to this study. The motor dysfunction scale was evaluated using the gross motor function classification system (GMFCS). Thirty-three patients had a mild degree of motor dysfunction (17 subjects with Level 1 and 16 subjects with Level 2), and 10 patients had moderate-to-severe dysfunction (Level 3 in six, Level 4 in three and Level 5 in one subject).

Conventional magnetic resonance imaging acquisition

For structural imaging, we obtained high-resolution T_1-weighted MRI volume data using a Philips 3T scanner (Intera Achieva, Philips Medical System, Best, The Netherlands) with a SENSE head coil. The scanning parameters of the 3D T1-TFE sequence were an axial acquisition with a 224×256 matrix, field of view = 220 mm, voxel size = $0.98 \times 0.98 \times 1.2\,mm^3$, echo time = 4.6 ms, repetition time = 9.6 ms, flip angle = 8° and slice gap = 0 mm. The T_2-weighted images were acquired axially with a 400×319 matrix, field of view = 230 mm, voxel size = $0.45 \times 0.45 \times 5\,mm^3$, echo time = 80 ms, repetition time = 3000 ms, flip angle = 90° and slice gap = 2 mm. The T_2-weighted and fluid attenuation inversion recovery images were acquired axially with a 352×238 matrix, field of view = 230 mm, voxel size = $0.45 \times 0.45 \times 5\,mm^3$, echo time = 125 ms, repetition time = 11 000 ms and slice gap = 2 mm.

Diffusion tensor image acquisition

We obtained diffusion tensor images using a single-shot echo-planar acquisition with the following parameters: 112×112 acquisition and a 128×128 reconstructed matrix, field of view = 220 mm, voxel size = $1.72 \times 1.72 \times 2\,mm^3$, SENSE factor 2, echo time = 70 ms; shortest repetition time = ~13 000 ms, flip angle = 90°, slice gap = 0 mm, two averages per slice, *b*-factor = $600\,s/mm^2$, non-cardiac gating and ~70 axial slices. We acquired diffusion-weighted images from 45 non-collinear, non-coplanar directions with a baseline image without diffusion weighting. The spatial distortions induced by eddy currents and motion artefacts in diffusion-weighted images were corrected by registering the diffusion-weighted images to the non-diffusion-weighted *b*0 image using a low order non-linear transformation (Kim *et al.*, 2006).

Resting state functional magnetic resonance imaging acquisition

Among the 43 patients, we performed resting state functional MRI in 13 subjects and obtained data from 11 (mean age of 10.17 ± 2.69 years); two subjects were excluded due to motion artefacts. Functional MRI data of age-matched normal controls ($n = 11$, mean age of 12.36 ± 4.13 years) without neurological and structural abnormalities; risk factors for periventricular leucomalacia were used for group comparison. We acquired 165 axial volume scans from each subject using a T_2-weighted single shot echo planar imaging sequence using a 3T Philips MRI scanner with the following parameters: voxel size = $2.75 \times 2.75 \times 4.8\,mm^3$, slice number = 29 (interleaved), matrix = 80×80, slice thickness = 4.8 mm, repetition time = 2000 ms, echo time = 30 ms, field of view = $209 \times 220\,mm^2$. Foam pads were used to reduce head motion during echo planar imaging data acquisition. During each scan, subjects were instructed to keep their eyes closed, rest without movement and attempt to sleep for ~5 min.

Tract-based spatial statistics of white matter fractional anisotropy

We performed statistical analysis of the fractional anisotropy values with a tract-based spatial statistics technique using FMRIB's Diffusion Toolbox implemented in the FMRIB's software library (http://www.fmrib.ox.ac.uk/fsl/tbss/index.html) as described previously (Smith *et al.*, 2006; Anjari *et al.*, 2007). A mean fractional anisotropy skeleton with a threshold fractional anisotropy >0.2 from all patients was generated to include the major white matter tracts. Fractional anisotropy data of age-matched normal controls ($n = 43$) without neurological and structural abnormalities or any risk factors for periventricular leucomalacia were derived from our normal database. The MRI acquisition methods used for normal controls were not different from those of patients. Fractional anisotropy differences between the patient and control group were evaluated with a permutation-based randomized test (Nichols *et al.*, 2002) and inference using threshold-free cluster enhancement (Smith *et al.*, 2009) implemented in FMRIB's software library to correct multiple comparison problems.

To investigate white matter injury sites that are associated with motor dysfunction, we performed voxelwise correlation analysis between fractional anisotropy values within the major white matter tracts and GMFCS levels using threshold-free cluster enhancement and results were obtained after 10 000 random permutations (nuisance parameters: age and sex). The voxels with significant correlation ($P < 0.05$, family-wise error corrected) were projected onto the mean fractional anisotropy skeleton on tract-based spatial statistics.

Assessment of white and grey matter volume reduction

The white matter volume was calculated after extraction of grey matter volume using Freesurfer software v.4.0.5 (http://surfer.nmr.mgh.harvard.edu). The white matter volume adjusted for intracranial volume (white matter volume/intracranial whole brain volume) was compared with GMFCS level after age correction.

We performed voxel-based morphometry in patient group and age- and gender-matched healthy controls ($n = 43$) using DARTEL (Ashburner, 2007) implemented in the Statistical Parametric Mapping 8 software (http://fil.ion.ucl.ac.uk/spm, Wellcome Department of Cognitive Neurology, London, UK). We generated a group grey matter template to which the entire individual grey matter segmentation map was spatially normalized. To adjust the volume changes during the non-linear transformations, spatially normalized grey matter segmentation maps were modulated by the amount of expansion or shrinkage during the spatial normalization process by applying the Jacobian determinant of the deformation field (Good *et al.*, 2001).

These modulated grey matter maps were smoothed using a 6 mm full-width half-maximum isotropic Gaussian kernel. The regional volume differences between spastic diplegic cerebral palsy subjects and healthy controls were determined using *t*-statistics for every voxel in the grey matter and correlation analysis between grey matter volumetric density of each voxel and GMFCS level was

performed in patients with spastic diplegic cerebral palsy using Statistical Parametric Mapping 8.

Resting state functional connectivity study

In consideration of the magnetization equilibrium, the first 10 images from the functional MRI data were excluded. The remaining 155 echo planar images were corrected for the acquisition time delay between different slices. We adjusted for head motions by realigning 155 consecutive volumes to the first image of the session. The realigned images were coregistered to T_1-weighted images that were used to spatially normalize functional data to a template space using non-linear transformation. The normalized data were then spatially smoothed using an 8 mm full-width half-maximum Gaussian filter.

Functional connectivity maps between motor cortex or thalami and whole brain grey matter were calculated using a correlation approach. The time series of each of the motor cortex and thalami were calculated by averaging the activity of the bilateral Brodmann area (BA) 4 for motor cortex, which was defined by the cytoarchitectonic map (Geyer *et al*., 1996), and by averaging the activity of the bilateral thalami in automated anatomical labelling (Tzourio-Mazoyer *et al*., 2002). Time series of all voxels within the grey matter were quadratic detrended and band-pass filtered (0.01–0.08 Hz) (Weissenbacher *et al*., 2009). For each subject, the correlation coefficients between time series of seed regions and those of each voxels within the grey matter were transformed to a *z*-value using Fisher *r–z* transformation (Weissenbacher *et al*., 2009). Statistical analysis of the motor cortical or thalamic connectivity map was performed by one sample *t*-test. The connectivity map between patients with spastic diplegic cerebral palsy and normal control groups was also compared using two-sample *t*-test with Statistical Parametric Mapping 8.

^{18}F-fluoroflumazenil positron emission tomography imaging and statistical analysis of binding potential using statistical parametric mapping

^{18}F-fluoroflumazenil used in this study is a newly developed radiotracer that binds to central benzodiazepine receptors. The B_{max}, K_d and IC_{50} values of this radiotracer are comparable to those of ^{3}H-flumazenil (Mitterhauser *et al*., 2004; Chang *et al*., 2005; Lee *et al*., 2007).

Twenty-seven patients (14 males and 13 females, mean age 13.89 ± 4.79 years, median 14 years) and 20 normal volunteers (10 males and 10 females, mean age 21.20 ± 1.32 years, median 21 years) completed a dynamic PET scan without motion artefact using a DSTe PET scanner (GE, Milwaukee, WI, USA) to measure the $GABA_A$ receptor binding potential. Among the 27 patients with spastic diplegic cerebral palsy, eight subjects (mean age 22.8 ± 4.09 years) were age-matched to normal controls. A transmission CT scan was performed for attenuation correction and dynamic emission data were obtained in a sequence of 150 frames in 3D mode (60 × 10 s, 40 × 15 s, 20 × 30 s, 30 × 60 s) for a total acquisition time of 60 min after injection of ~5.5 MBq (0.15 mCi)/kg of ^{18}F-fluoroflumazenil. The attenuation corrected images were reconstructed in a 128 × 128 × 35 matrix with a voxel size of 1.95 × 1.95 × 4.25 mm using the Hanning and Ramp filters.

To calculate the $GABA_A$ receptor binding potential, we used a multi-linear reference tissue method (Millet *et al*., 2002) that was implemented in PMOD software (PMOD Technologies Ltd., Zurich, Switzerland). The mean activity within a manually delineated the region of interest at the pons was used for reference tissue activity because the density of $GABA_A$ receptors in the pons is negligible.

Spatial pre-processing and statistical analysis of the ^{18}F-fluoroflumazenil PET data were performed using Statistical Parametric Mapping 8 for the group comparison of the binding potential map. The $GABA_A$ receptor binding potential data of the patient group (n = 27) and the age-matched subgroup of patients with spastic diplegic cerebral palsy (n = 8) were compared with those of normal control group after scaling the binding potential map images proportionally by the global whole brain $GABA_A$ receptor binding potential. Proportional scaling was performed to minimize the individual variation of the global binding potential resulted from wide range of age distribution in patient group. This study was conducted in accordance with institutional guidelines and was approved by the institutional review board (No. 4-2006-0311). We obtained informed consent from all subjects and normal controls.

Results

White matter injury in patients with spastic diplegic cerebral palsy

Conventional MRI showed various degrees of ventricular dilatation and decreased white matter volume, mainly within the posterior thalamic radiation, posterior part of the corona radiata and thinning of corpus callosum in all patients with spastic diplegic cerebral palsy (Fig. 1A). However, increased signal intensity representing white matter injury extended almost to the entire bilateral periventricular white matter regions including the anterior portion of the corona radiata on fluid attenuated inversion recovery images (Fig. 1B and C). Group comparison of fractional anisotropy values between patients with spastic diplegic cerebral palsy and healthy controls using tract-based spatial statistics revealed lower fractional anisotropy values within almost all white matter tracts in the patient group, although white matter tracts within the posterior part of the brain were more extensively involved than anterior white matter tracts (Fig. 1D, $P < 0.05$ family-wise error corrected).

Correlation of the severity of white matter injury with GMFCS levels

White matter volume reduction in each hemisphere did not show significant correlation with motor dysfunction ($P > 0.1$). Fractional anisotropy values within the posterior white matter tracts and corpus callosum showed a negative correlation with GMFCS levels ($P < 0.05$ family-wise error corrected). However, fractional anisotropy values within the bilateral corticospinal tracts and posterior body of the corpus callosum were more strongly correlated with motor dysfunction ($P < 0.03$ family-wise error corrected) (Fig. 2).

Grey matter injury on voxel-based morphometry

Grey matter volume of the bilateral sensorimotor cortex, parietal, temporal and occipital lobes, posterior cingulate cortex, basal ganglia, thalami and cerebellum was significantly reduced in the

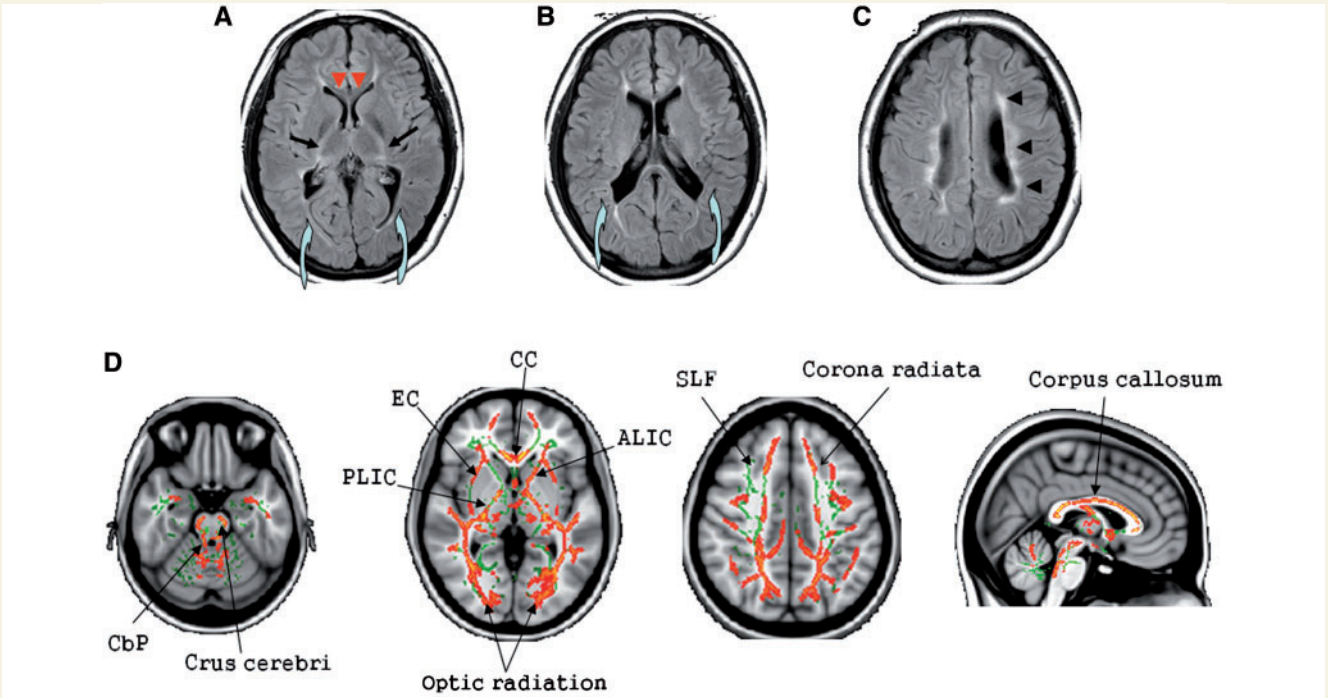

Figure 1 Periventricular white matter injury in patients with periventricular leucomalacia on conventional MRI and tract-based spatial statistics. (**A–C**) Transaxial fluid attenuated inversion recovery images show dilatation of the lateral ventricles with angular deformity of the lateral margins, approximation of the grey matter and sulci to the ventricular margins secondary to white matter volume loss (curved arrows) and thinning of the corpus callosum (red arrow heads). These are typical MRI findings of diffuse type periventricular leucomalacia. Increased signal intensity, representing white matter injury, can be seen within the posterior limb of the internal capsule (black arrows) and also within the periventricular white matter regions. Periventricular white matter injury is present not only within the posterior corona radiata but also within the anterior corona radiata (black arrow heads). (**D**) Group comparison of fractional anisotropy values between patients with periventricular leucomalacia and age-matched healthy controls using tract-based spatial statistics shows decreased fractional anisotropy values in almost all major white matter tracts. Regions of the mean fractional anisotropy skeleton in green represent undamaged tracts, while regions in red represent damaged white matter tracts in patient group ($P < 0.05$, family-wise error corrected). ALIC = anterior limb of the internal capsule; CbP = cerebellar peduncle; CC = corpus callosum; EC = external capsule; PLIC = posterior limb of the internal capsule; SLF = superior longutudinal fascicle.

patient group compared with the age- and gender-matched normal controls (Fig. 3A, $P < 0.005$ false discovery rate corrected). In particular, cortical volume of the pre- and post-central gyri, and the paracentral lobule tended to be negatively correlated with GMFCS levels at the threshold level of uncorrected $P < 0.005$ ($q < 0.22$ after false discovery rate control) (Fig. 3B).

Motor cortical and thalamic connectivity

The motor cortex in normal control subjects had extensive functional connections to the adjacent somatosensory cortex, visual cortex and cerebellum on one-sample *t*-test. In the patient group, motor cortical connections appeared to have connections more expanded to the adjacent parietal area (family-wise error corrected $P < 0.05$). However, group comparison study showed decreased connectivity within the bilateral somatosensory cortex, paracentral lobule, presupplementary motor area, cingulate motor area, visual cortex, superior and inferior parietal lobules in the patient group at the threshold level of uncorrected $P < 0.005$ ($q < 0.06$ after false discovery rate control) (Fig. 4A).

Thalami are connected to the basal ganglia, cerebellum and overlying cortex especially to the cingulate cortex in normal controls. In the patient group, parietal, occipital, prefrontal and posterior cingulate connectivity appeared to be more expanded on one-sample *t*-test ($P < 0.05$, family-wise error corrected). A group comparison study showed that thalamic connectivity to the caudate nucleus, anterior and posterior cingulate cortex, and cerebellum appeared to be diminished in patient group at the threshold level of uncorrected $P < 0.005$ ($q < 0.11$ after false discovery rate control) (Fig. 4B). Thalamo-visual connectivity was not affected despite severe optic radiation damage.

Statistical analysis of $GABA_A$ receptor binding potential

$GABA_A$ receptor binding potential was focally increased within the bilateral lower extremity homunculus including the paracentral lobule, cingulate cortex, visual cortex and cerebellum despite significant grey matter volume reduction, whereas receptor binding potential was diffusely decreased in the prefrontal, temporal,

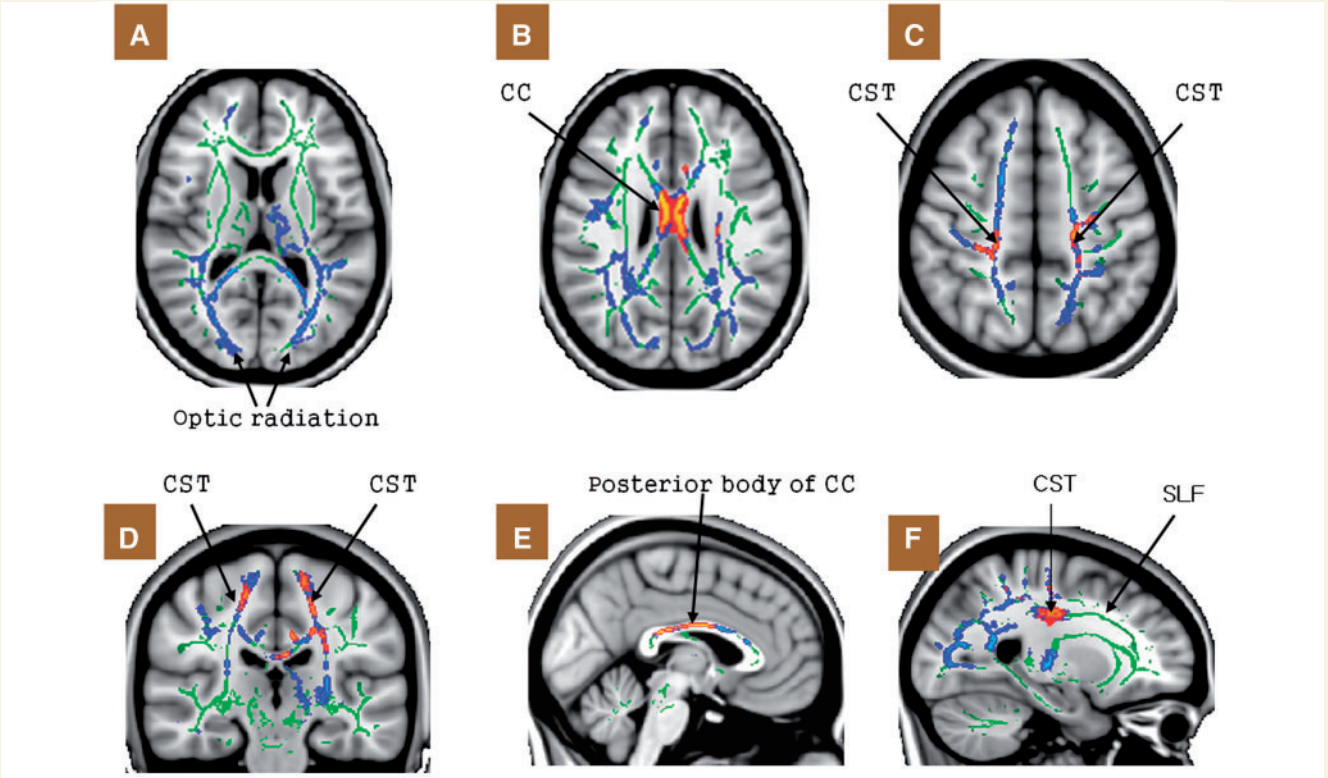

Figure 2 Voxel-wise correlation analysis between fractional anisotropy values and GMFCS levels on tract-based spatial statistics. Green lines represent a mean fractional anisotropy skeleton of undamaged white matter tracts. Areas in blue represent regions showing significant negative correlation between fractional anisotropy values and GMFCS levels ($P < 0.05$, family-wise error corrected). Fractional anisotropy values of most of the white matter tracts within the posterior brain areas show a significant negative correlation with GMFCS levels (**A–C**). In particular, fractional anisotropy values within the bilateral corticospinal tracts (**C–F**) and the posterior body of the corpus callosum (**E**) also show significant correlation with motor dysfunction (red clusters, $P < 0.03$, family-wise error corrected). CC = corpus callosum; CST = corticospinal tract; SLF = superior longitudinal fascicle.

parietal and subcortical nuclei in patient group (Fig. 5, $P < 0.05$, false discovery rate corrected) (Table 1). Group comparison study between the age-matched spastic diplegic cerebral palsy subgroup ($n = 8$) and normal control group confirmed increased receptor binding pattern within these regions as seen in the total patient group (Fig. 6).

Discussion

The diffuse form of periventricular leucomalacia is known to be a leading aetiological factor of cerebral palsy, especially in infants with very low birth weight or those born prematurely (Bax *et al*., 2006; Platt *et al*., 2007). The underlying pathophysiological mechanisms of diffuse periventricular leucomalacia include hypoxic-ischaemic insult with excessive glutamatergic excitotoxicity and free radical injury to the immature oligodendrocytes or oligodendrocyte precursor cells. Maternal-fetal infections (Rezaie and Dean, 2002; Back *et al*., 2007) or chorioamnionitis are independent risk factors for cerebral palsy as well as leading causes of periventricular leucomalacia (Wu *et al*., 2003).

The severity of white matter injury as seen on conventional MRI is considered to be closely correlated with motor dysfunction in patients with periventricular leucomalacia. However, this relationship is still debatable since patients with periventricular leucomalacia do not always have neurological abnormalities, and structural abnormalities may not be seen on conventional MRI in patients with spastic diplegic cerebral palsy (Olsen *et al*., 1997). In addition, it is still controversial whether corticospinal tract injury is related to motor dysfunction in patients with periventricular leucomalacia and spastic diplegic cerebral palsy. Previous reports demonstrated a significant correlation of corticospinal tract injury with neurological impairments (Kidokoro *et al*., 2008; Murakami *et al*., 2008), whereas Hoon *et al*. (2009) reported that motor dysfunction is more related to thalamocortical injury with abnormal sensorimotor connections rather than corticospinal tract injury itself. Therefore, pathophysiological mechanisms involved in motor impairment in patients with periventricular leucomalacia need to be further elucidated. However, these controversial results might have been resulted from limitations of the analytic method used; conventional MRI technique is not sensitive to detect subtle white matter injury and it is also difficult to identify individual white matter tract injury precisely, in particular, corticospinal tract

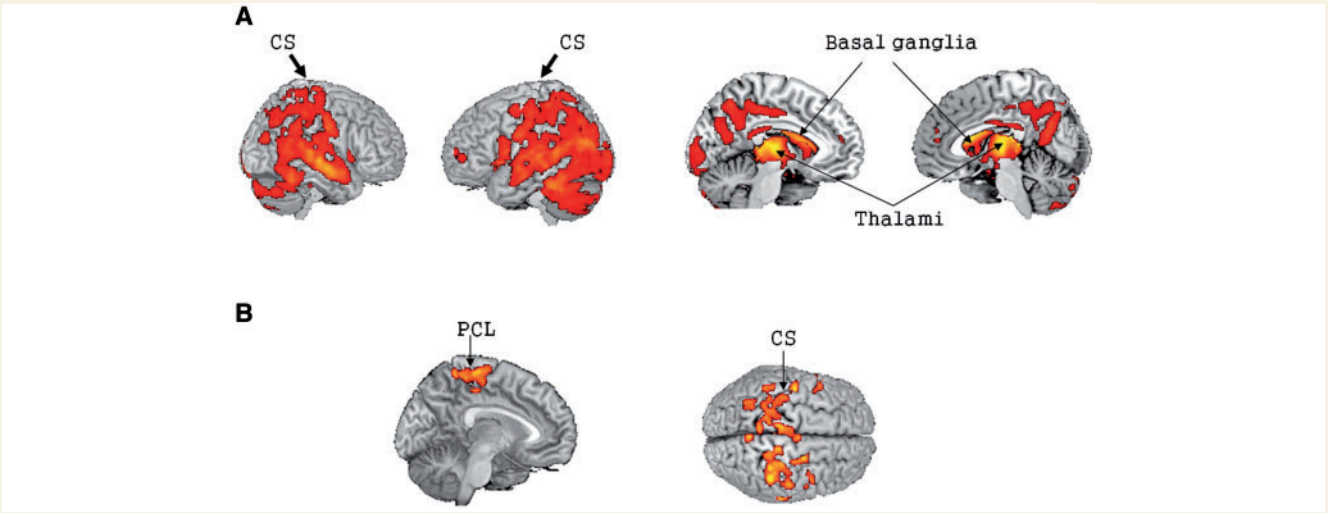

Figure 3 Grey matter volume reduction in patients with periventricular leucomalacia and correlation with motor dysfunction. (**A**) Voxel-based morphometry. Grey matter volume is reduced mainly within the posterior part of the cerebral cortex including the sensorimotor cortex, basal ganglia and thalami in patients with periventricular leucomalacia ($P < 0.005$, false discovery rate corrected, cluster size $\geqslant 100$). (**B**) Grey matter volume reduction versus motor dysfunction. Grey matter volume within the pre- and post-central gyri and paracentral lobule is negatively correlated with GMFCS levels (uncorrected $P < 0.005$ or $q < 0.22$ after false discovery rate control, cluster size $\geqslant 100$). CS = central sulcus; PCL = paracentral lobule.

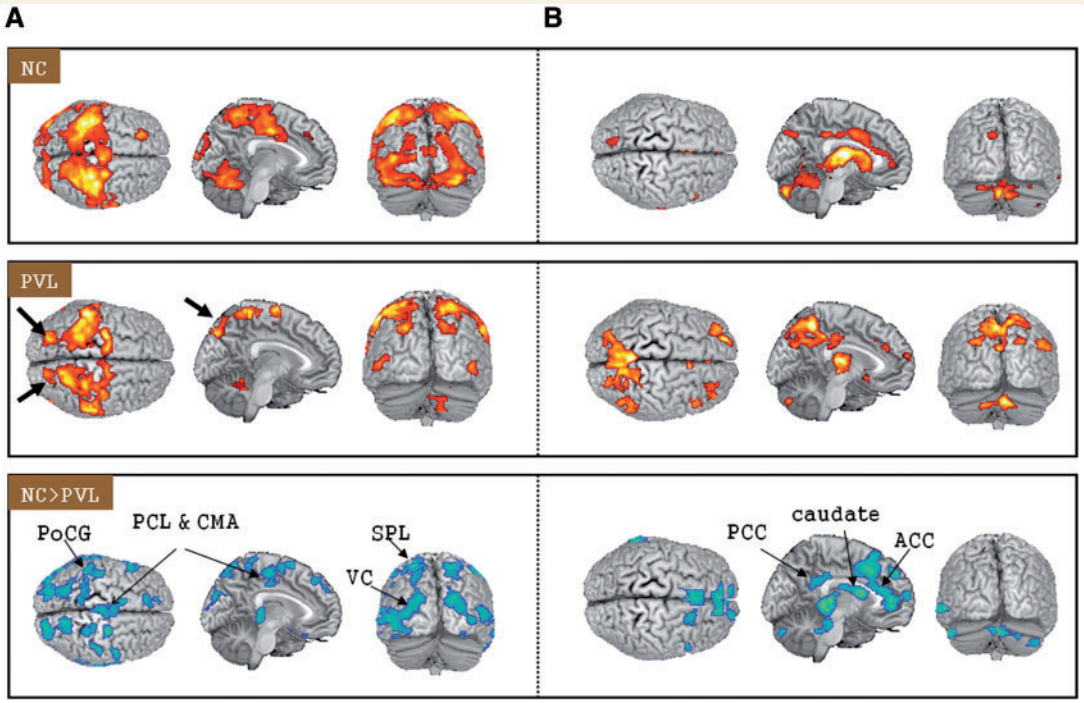

Figure 4 Functional connectivity of the motor cortex and thalami. (**A**) Motor connectivity. The patient group shows more expanded motor cortical connections to the adjacent parietal area on one-sample *t*-test (arrows, $P < 0.05$, family-wise error corrected, cluster size $\geqslant 100$). However, group comparison revealed decreased sensorimotor and visuomotor connections in patient group (uncorrected $P < 0.005$, or $q < 0.06$ after false discovery rate control). (**B**) Thalamic connectivity to the parieto-occipital area, cingulate cortex and frontal area appears to be more expanded in patient group based on one-sample *t*-test ($P < 0.05$, family-wise error corrected, cluster size $\geqslant 100$); however, connectivity is decreased within the cingulate cortex and the caudate nucleus on group comparison (uncorrected $P < 0.005$, or $q < 0.12$ after false discovery rate control). ACC = anterior cingulate cortex; CMA = cingulate motor area; PCC = posterior cingulate cortex; PCL = paracentral lobule; PoCG = post-central gyrus; VC = visual cortex; SPL = superior parietal lobule.

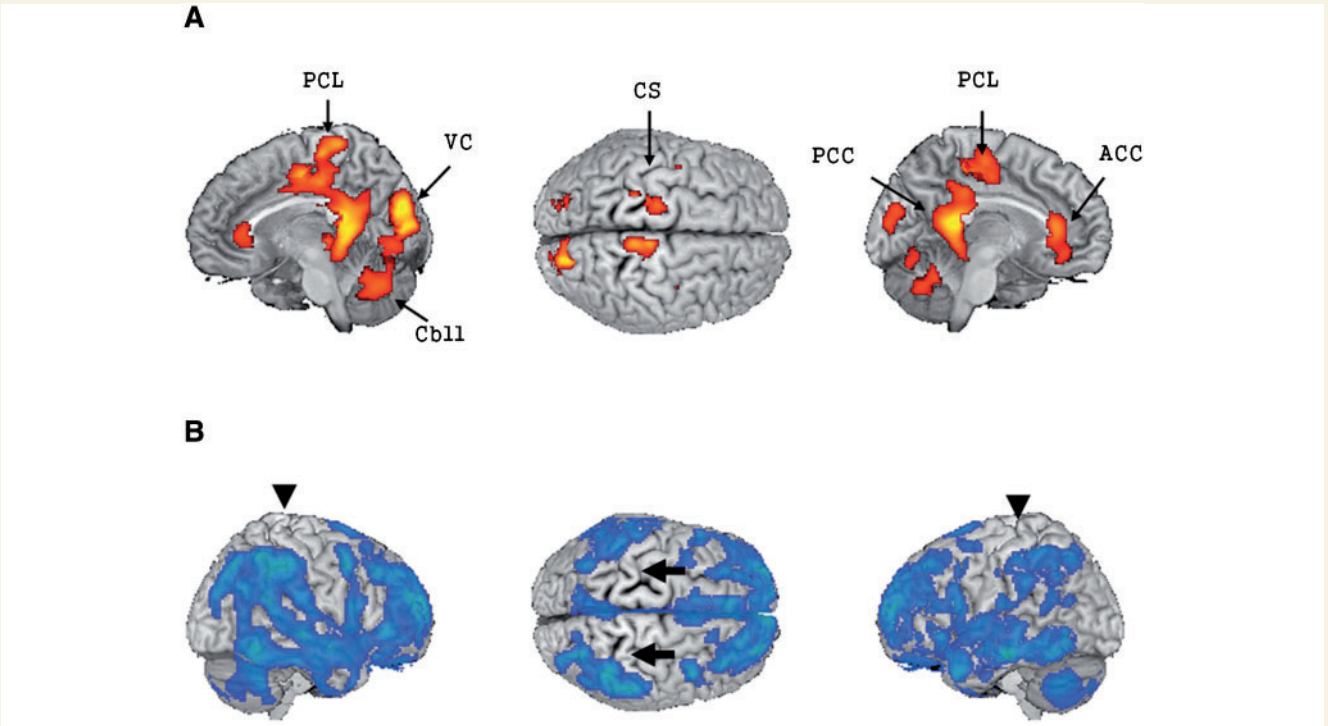

Figure 5 $GABA_A$ receptor binding pattern in patients with periventricular leucomalacia and spastic diplegic cerebral palsy compared with healthy controls. (**A**) The $GABA_A$ receptor binding potential is focally increased within the paracentral lobule, lower extremity honunculus, cingulate cortex, visual cortex and cerebellum in patient group (red colours, $P < 0.05$, false discovery rate corrected). (**B**) The $GABA_A$ receptor binding potential is diffusely decreased within the prefrontal, parietal, temporal and subcortical nuclei (blue colour, $P < 0.05$, false discovery rate corrected). Arrow heads and arrows denote central sulcus. ACC = anterior cingulate cortex; CS = central sulcus; Cbll = cerebellum; PCC = posterior cingulate cortex; PCL = paracentral lobule; VC = visual cortex.

injury. Although diffusion tensor imaging with tractography enables correct localization of individual tract injury, most of the previous results were derived from region of interest based analysis method, which is less sensitive than voxelwise analysis.

Recently, tract-based spatial statistics is being widely used for voxelwise group comparison of white matter diffusion properties for correlation analysis between white matter micro-structural abnormalities on diffusion tensor imaging and various functional abilities (Counsell *et al*., 2008). We compared group difference of fractional anisotropy values between patients with spastic diplegic cerebral palsy and controls using tract-based spatial statistics, and further analysed correlation between motor function scales and fractional anisotropy values at every voxel along the whole white matter tract trajectories. In the current study, fractional anisotropy values within most of the white matter tracts were significantly lower in patients with periventricular leucomalacia than those of age-matched normal controls ($P < 0.05$, family-wise error corrected). Although the severity of white matter injury within most of the posterior white matter tracts and corpus callosum showed a significant negative correlation with motor function ($P < 0.05$, family-wise error corrected), bilateral corticospinal tract injury and corpus callosal injury (posterior body) were more significantly correlated with motor dysfunction ($P < 0.03$, family-wise error corrected) (Fig. 2). These diffusion tensor imaging results clearly demonstrate that focal injury within the corticospinal tract is closely related to motor dysfunction in patients with periventricular leucomalacia. Negative correlation between GMFCS level and the severity of white matter injury within the posterior body and isthmus of the corpus callosum is also congruent with previous diffusion tensor imaging data showing close correlation with neurodevelopmental abilities (Counsell *et al*., 2008). In fact, these callosal regions are pathways for interconnecting the bilateral motor cortex (Park *et al*., 2008).

Grey matter injury such as neuronal degeneration, gliosis (Inder *et al*., 1999, 2005; Northington *et al*., 2005; Pierson *et al*., 2007; Stone *et al*., 2008) and subplate neuronal damage (Leviton and Gressens, 2007) is known to be commonly associated with periventricular leucomalacia following prenatal hypoxic-ischaemic insult. These neuronal injuries produce regional volume reduction and the geographic pattern of neuronal damage is close to the predilection sites of white matter injury, predominantly involving the posterior brain region (Leviton and Gressens, 2007) as shown on our voxel-based morphometry and tract-based spatial statistics studies. Although grey matter volume can be reduced within the predilection site of periventricular leucomalacia even in adolescents born very prematurely without motor disabilities (Nosarti *et al*., 2008), we found that cortical volume of the specific regions, especially somatosensory and motor cortices, and paracentral lobule appeared to be negatively correlated with GMFCS levels (Fig. 3). Therefore, our correlation analysis between grey matter volume

reduction and GMFCS levels along with the current fractional anisotropy correlation analysis data support the fact that motor pathway injury could be a leading pathophysiological mechanism of motor dysfunction in patients with periventricular leucomalacia since fibres of the corticospinal tract arise from the precentral and postcentral gyri including the paracentral lobule, premotor and parietal areas.

In addition to the morphological abnormalities, alteration of functional connectivity within the affected cortical areas could be an important determinant for final motor function. In a previous animal study, increased cortico-cortical connections within the visual cortex were observed after deafferentation of thalamocortical inputs (Kingsbury *et al*., 2002), and a human study demonstrated expanded sensorimotor cortical connections in patients with spastic diplegic cerebral palsy (Burton *et al*., 2009). Despite local expansion of the cortico-cortical connectivity, our patient group showed a diminished motor cortical connectivity especially within the bilateral paracentral lobule and cingulate motor area as compared with the age-matched control group. Sensory-motor and visuomotor connections, thalamic connections to the caudate nuclei and cingulate cortex were also diminished in the patient group. Based on these results, diminished motor cortical connectivity within the motor control areas, along with focal injury in the corticospinal tracts could be a relevant pathophysiological mechanism producing motor dysfunction. Although thalamic connectivity to the anterior cingulate cortex is diminished, it might be more related to impaired cognitive function in patients with spastic diplegic cerebral palsy. Further studies of the correlation between cognitive function scales and anterior cingulate connectivity are required.

Table 1 Increased $GABA_A$ receptor binding potential sites in spastic diplegic cerebral palsy ($P < 0.05$, false discovery rate corrected, cluster $\geqslant$100)

Side	Region	Brodmann area	MNI (mm)			Z_{max}
			x	y	z	
Right	Anterior cingulate	BA 24	10	32	6	3.70
	Posterior cingulate	BA 29	10	−42	12	5.07
	Cingulate gyrus	BA 24	12	−16	36	3.52
	Lingual gyrus	BA 18	26	−86	4	5.11
	Cuneus	BA 19	26	−82	16	5.42
	Fusiform gyrus	BA 20	36	−72	−4	4.85
	Paracentral lobule	BA 6	12	−28	62	4.78
	Precentral gyrus	BA 4	12	−28	62	5.38
	Insula	BA 13	44	−42	20	5.18
	Cerebellar tonsil	*	18	−60	−42	3.88
	Declive of vermis	*	2	−70	−20	3.39
Left	Anterior cingulate	BA 24	−2	28	10	4.40
	Posterior cingulate	BA 29	−6	−46	4	4.96
	Cingulate gyrus	BA 31	−16	−20	42	3.32
	Lingual gyrus	BA 18	−14	−90	6	3.84
	Cuneus	BA 19	−18	−82	14	3.84
	Fusiform gyrus	BA 20	−22	−88	−12	4.02
	Medial frontal gyrus	BA 6	−14	−24	56	3.76
	Precentral gyrus	BA 4	−26	−20	48	3.26
	Insula	BA 13	−40	−44	20	3.23
	Superior temporal gyrus	BA 41	−42	−42	6	4.01
	Cerebellar tonsil	*	−24	−52	−46	3.75

* = not applicable.

In terms of alterations in functional connectivity in patients with spastic diplegic cerebral palsy, it could be resulted from subplate neuronal injury following hypoxic-ischaemic insult with subsequent repairing process (Kingsbury *et al*., 2002; Burton *et al*., 2009) since subplate neurons are highly vulnerable to hypoxic-ischaemic insult (McQuillen and Ferriero, 2005; Leviton and Gressens, 2007). Under normal circumstances, subplate neurons receive inputs from the thalamus and send excitatory glutamatergic projection to cortical layer IV before cortical neurons directly receive thalamocortical inputs (Pinon *et al*., 2009; Kanold and Luhmann, 2010). When subplate neurons are damaged before maturation of the thalamocortical circuit, these projections bypass the injured areas, but project to the adjacent areas containing intact subplate neurons (Ghosh *et al*., 1990). In addition, descending cortical connections to the internal capsule, corpus callosum and deep subcortical nuclei also can be injured after subplate neuronal damage (De Carlos and O'Leary, 1992; McConnell *et al*., 1994).

After subplate neuronal injury, expression of the genes or proteins involved in neurotransmitter regulation, neuronal survival or axon extension is subsequently altered (Lein *et al*., 1999; Osheroff *et al*., 2009). Among the various neurotrophins and

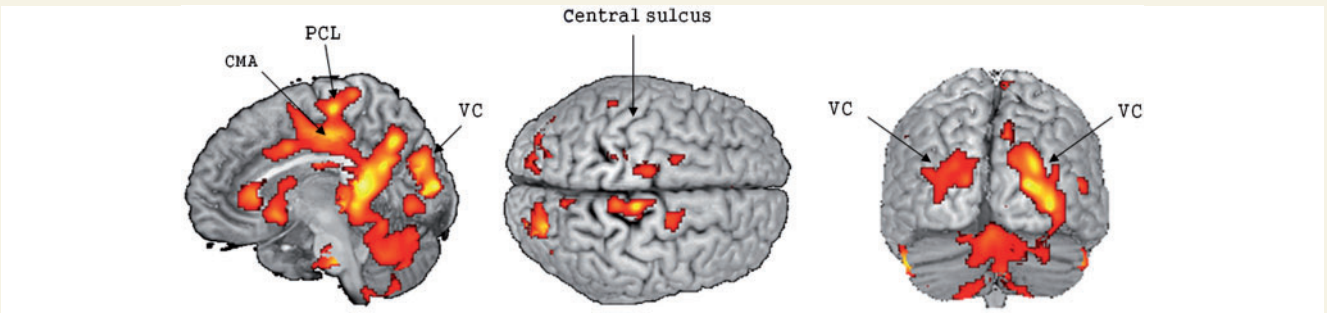

Figure 6 $GABA_A$ receptor binding pattern in age-matched patient subgroup ($n = 8$) compared with normal control group. The receptor binding pattern is almost the same as the binding pattern of the total patient group (uncorrected $P < 0.05$). CMA = cingulate motor area; PCL = paracentral lobule; VC = visual cortex.

neurotransmitters, we focused on $GABA_A$ receptor expression because inhibitory $GABA_A$ receptor plays a substantial role in brain remodelling processes after injury (Schwartz-Bloom and Sah, 2001). Usually, regional $GABA_A$ receptors within the ischaemic regions are transiently down-regulated or internalized into the cytoplasm (Schwartz-Bloom and Sah, 2001). Reduction of the inhibitory $GABA_A$ receptor expression is necessary to induce or maintain the excitability of perilesional and functionally connected neurons and to expand receptive field size for an optimal practice-dependent plasticity (Pascual-Leone *et al*., 2005; Benali *et al*., 2008; Cramer, 2008). In fact, long-term decreased uptake of ^{11}C-flumazenil within the damaged areas after ischaemia has been reported previously (Yamauchi *et al*., 2007).

A post-mortem human study also revealed significant loss of GABAergic neurons and $GABA_A$ receptor density within the prefrontal cortex in infants with periventricular leucomalacia (Robinson *et al*., 2006). In the current study, the patients with spastic diplegic cerebral palsy group showed decreased $GABA_A$ receptor binding potential within the prefrontal, parietal and temporal areas as previous reported. In contrast, receptor binding potential was focally increased within the lower extremity homunculus, cingulate cortex, visual cortex and cerebellum despite significant grey matter volume reduction (Fig. 5). Our previous report using delayed PET images also demonstrated a significant higher uptake of ^{18}F-fluoroflumazenil within the bilateral motor and visual cortices in patients with spastic diplegic cerebral palsy (Lee *et al*., 2007). However, focally increased $GABA_A$ receptor binding potential, especially within the motor control areas, is contradictory to the classical GABAergic response to ischaemic insult, and also contradictory to radiolabelled flumazenil uptake pattern within ischaemic areas because the uptake of radiolabelled central benzodiazepine receptor agents within damaged neurons is decreased (Yamauchi *et al*., 2007). Our contradictory results could be explained by the fact that immature forms of the $GABA_A$ receptors consisting of $\alpha2$ and $\alpha3$ subunits with a depolarizing activity are upregulated after prenatal ischaemic injury until adulthood, whereas mature form $\alpha1$ subunits of $GABA_A$ receptors are down-regulated (Paysan *et al*., 1997; Kanold and Shatz, 2006; Kanold and Luhmann, 2010). Therefore, we hypothesized that $GABA_A$ receptors were upregulated in patients with spastic diplegic cerebral palsy as an adaptive neuronal plasticity process in compensation for reduced GABAergic neuronal input and diminished functional connectivity due to white matter injury or overlying grey matter volume reduction or both. Further studies regarding to the subunit composition of the $GABA_A$ receptors and their function are required.

Limitations of the study

This study has several limitations. First, resting state functional MRI data were obtained from only 11 patients and majority of our patients with spastic diplegic cerebral palsy had lower GMFCS levels, which might result in low statistical power for group comparison of motor and thalamic connectivity between normal controls and patients with spastic diplegic cerebral palsy (uncorrected $P < 0.005$). However, the threshold of uncorrected $P < 0.005$ is estimated to be $q < 0.06$ for motor and $q < 0.11$ for thalamic connectivity, respectively, after false discovery rate control. Therefore, statistical significance of our group comparison data in functional connectivity study can be acceptable since q-value in the range 0.1–0.2 after false discovery rate control is known to be acceptable for multiple comparison (Genovese *et al*., 2002). Future works with a large series of patient group would produce better results with higher statistical power.

Second, our patients with spastic diplegic cerebral palsy group had a wide range of age distribution. However, it would not significantly affect on our results since cerebral palsy is a permanent and non-progressive disorder (O'Shea, 2008). Nevertheless, further studies with a narrow age range patient group are needed.

Another limitation may be diffusion tensor imaging data acquisition errors due to motion artefact. In this study, we obtained diffusion-weighted images from 45 directions to increase the tensor estimation reliability of the tensor estimation (Jones *et al*., 2004). Although this acquisition method might produce motion artefacts, we used a low order non-linear transformation between diffusion-weighted images and the *b*0 image to reduce motion artefacts as well as eddy current effects (Kim *et al*., 2006). Therefore, statistical results in the current study might not be significantly affected by tensor estimation errors.

Conclusion

Our data demonstrate that descending motor pathways injury along with overlying cortical volume reduction and decreased functional connectivity could be a leading pathophysiological mechanism for motor dysfunction in patients with periventricular leucomalacia. The severity of optic radiation injury was less correlated with motor impairment than corticospinal tract injury. Increased $GABA_A$ receptor binding potential, especially within the decreased connectivity areas could be related to compensatory plasticity process after brain injury.

Acknowledgements

We thank Mr Hoon Hee Park, Han Sang Lim, Dong Wook Rho and Hyuk Namgung for their excellent technical assistance in data acquisition and processing; Drs Jung Young Kim and Tae Hyun Choi for the production of ^{18}F-fluoroflumazenil. The production techniques and the quality control of ^{18}F-fluoroflumazenil were supported by the Korea Institute of Radiological and Medical Sciences project.

Funding

Korea Healthcare Technology R&D Project, Ministry for Health, Welfare and Family Affairs, Republic of Korea (A080446).

References

Anjari M, Srinivasan L, Allsop JM, Hajnal JV, Rutherford MA, Edward AD, et al. Diffusion tensor imaging with tract-based spatial

statistics reveals local white matter abnormalities in preterm infants. Neuroimage 2007; 35: 1021–7.
Arzoumanian Y, Mirmiran M, Barnes PD, Woolley K, Ariagno RL, Mosely ME, et al. Diffusion tensor brain imaging findings at term-equivalent age may predict neurologic abnormalities in low birth weight preterm infants. Am J Neuroradiol 2003; 24: 1646–53.
Ashburner J. A fast diffeomorphic image registration algorithm. Neuroimage 2007; 38: 95–113.
Back SA, Riddle A, McClure MM. Maturation-dependent vulnerability of perinatal white matter in premature birth. Stroke 2007; 38 (2 Suppl): 724–30.
Bax M, Tydeman C, Flodmark O. Clinical and MRI correlates of cerebral palsy: the European Cerebral Palsy Study. JAMA 2006; 296: 1602–8.
Benali A, Weiler E, Benali Y, Dinse HR, Eysel UT. Excitation and inhibition jointly regulate cortical reorganization in adult rats. J Neurosci 2008; 28: 12284–93.
Burton H, Dixit S, Litkowski P, Wingert JR. Functional connectivity for somatosensory and motor cortex in spastic diplegia. Somatosens Mot Res 2009; 26: 90–104.
Chang YS, Jeong JM, Yoon YH, Kang WJ, Lee SJ, Lee DS, et al. Biological properties of 2′-[18F]fluoroflumazenil for central benzodiazepine receptor imaging. Nucleic Med Biol 2005; 32: 263–8.
Counsell SJ, Edward AD, Chew ATM, Anjari M, Dyet LE, Srinvasan L, et al. Specific relations between neurodevelopmental abilities and white matter microstructure in children born preterm. Brain 2008; 131: 3201–8.
Cramer SC. Repairing the human brain after stroke: I. Mechanisms of spontaneous recovery. Ann Neurol 2008; 63: 272–87.
Dale AM, Fischl B, Sereno MI. Cortical surface-based analysis. I. Segmentation and surface reconstruction. Neuroimage 1999; 9: 179–94.
De Carlos JA, O'Leary DDM. Growth and targeting of subplate axons and establishment of motor cortical pathways. J Neurosci 1992; 12: 1194–211.
Genovese CR, Lazar NA, Nichols T. Thresholding of statistical maps in functional neuroimaging using the false discovery rate. Neuroimage 2002; 15: 870–8.
Geyer S, Ledberg A, Schleiche A, Kinomura S, Schormann T, Burgel U, et al. Two different areas within the primary motor cortex of man. Nature 1996; 382: 805–7.
Ghosh A, Antonini A, McConnell SK, Shatz CJ. Requirement for subplate neurons in the formation of thalamocortical connections. Nature 1990; 347: 179–81.
Good CD, Johnsrude IS, Ashburner J, Henson RN, Friston KJ, Frackowiak RS A. Voxel-based morphometric study of ageing in 465 normal adult human brains. Neuroimage 2001; 14: 21–36.
Hoon AH, Stashinko EE, Nagae LM, Lin DD, Keller J, Bastian A. Sensory and motor deficits in children with cerebral palsy born preterm correlates with diffusion tensor imaging abnormalities in thalamocortical pathways. Dev Med Child Neurol 2009; 51: 697–704.
Inder TE, Huppi PS, Warfield S, Kikinis R, Zientara GP, Barnes PD. Periventricular white matter injury in the premature infant is followed by reduced cerebral cortical gray matter volume at term. Ann Neurol 1999; 46: 755–60.
Inder TE, Warfield SK, Wang H, Huppi PS, Volpe JJ. Abnormal cerebral structure is present at term in premature infants. Pediatrics 2005; 115: 286–94.
Jones DK. The effect of gradient sampling schemes on measures derived from diffusion tensor MRI: a Monte Carlo study. Magn Reson Med 2004; 51: 807–15.
Kanold PO, Shatz CJ. Subplate neurons regulate maturation of cortical inhibition and outcome of ocular dominance plasticity. Neuron 2006; 51: 627–38.
Kanold PO, Luhmann HJ. The subplate and early cortical circuits. Ann Rev Neurosci 2010;in press (doi:10.1146/annurev-neuron-060909-153244).
Kidokoro H, Kubota T, Ohe H, Hattori T, Miyajima Y, Ogawa A, et al. Diffusion-weighted magnetic resonance imaging in infants with periventricular leukomalacia. Neuropediatrics 2008; 39: 233–8.
Kim DJ, Park HJ, Kang KW, Shin YW, Kim JJ, Moon WJ, et al. How does distortion correction correlate with anisotropic indices? A diffusion tensor imaging study. Magn Reson Imaging 2006; 24: 1369–76.
Kingsbury MA, Lettman NA, Finlay BL. Reduction of early thalamic input alters adult corticocortical connectivity. Brain Res Dev Brain Res 2002; 138: 35–43.
Lee JD, Park HJ, Park ES, Kim DG, Rha DW, Kim EY, et al. Assessment of regional GABA(A) receptor binding using 18F-fluoroflumazenil positron emission tomography in spastic type cerebral palsy. Neuroimage 2007; 34: 19–25.
Lein ES, Finney EM, McQuillen PS, Shats CJ. Subplate neuron ablation alters neurotrophin expression and ocular dominance column formation. Proc Natl Acad Sci USA 1999; 96: 13491–5.
Leviton A, Gressens P. Neuronal damage accompanies perinatal white-matter damage. Trends Neurosci 2007; 30: 473–8.
McConnell SK, Ghosh A, Shatz CJ. Subplate pioneers and the formation of descending connections from cerebral cortex. J Neurosci 1994; 14: 1892–907.
McQuillen PS, Ferriero DM. Perinatal subplate neuron injury: implications for cortical development and plasticity. Brain Pathol 2005; 15: 250–60.
Millet P, Graf C, Buck A, Walder B, Ibanez V. Evaluation of the reference tissue models for PET and SPECT benzodiazepine binding parameters. Neuroimage 2002; 17: 928–42.
Mitterhauser M, Wadsak W, Wabnegger L, Mien LK, Togel S, Langer O, et al. Biological evaluation of 2′-[18F]fluoroflumazenil ([18F]FFMZ), a potential GABA receptor ligand for PET. Nucl Med Biol 2004; 31: 291–5.
Murakami A, Morimoto M, Yamada K, Kizu O, Nishimura A, Nishimura T, et al. Fiber-tracking techniques can predict the degree of neurologic impairment for periventricular leukomalacia. Pediatrics 2008; 122: 500–6.
Nichols TE, Holmes AP. Nonparametric permutation tests for functional neuroimaging: a primer with examples. Hum Brain Map 2002; 15: 1–25.
Northington FJ, Graham EM, Martin LJ. Apoptosis in perinatal hypoxic-ischemic brain injury: how important is it and should it be inhibited? Brain Res Brain Res Rev 2005; 50: 244–57.
Nosarti C, Giouroukou E, Healy E, Rifkin L, Walshe M, Reichenberg A, et al. Gray and white matter distribution in very preterm adolescents mediates neurodevelopmental outcome. Brain 2008; 131: 205–17.
Olsen P, Paakko E, Vainionpaa L, Pyhtinen J, Jarvelin MR. Magnetic resonance imaging of periventricular leukomalacia and its clinical correlation in children. Ann Neurol 1997; 41: 754–61.
O'Shea M. Cerebral palsy. Semin Perinatol 2008; 32: 35–41.
Osheroff H, Hatten ME. Gene expression profiling of preplate neurons destined for the subplate: genes involved in transcription, axon extension, neurotransmitter regulation, steroid hormone signaling, and neuronal survival. Cereb Cortex 2009; 19: 1126–34.
Park HJ, Kim JJ, Lee SK, Seok JH, Chun J, Kim DI, et al. Corpus callosal connection mapping using cortical gray matter parcellation and DT-MRI. Hum Brain Mapp 2008; 29: 503–16.
Pascual-Leone A, Amedi A, Fregni F, Merabet LB. The plastic human brain cortex. Annu Rev Neurosci 2005; 28: 377–401.
Paysan J, Kossel A, Bolz J, Fritschy JM. Area-specific regulation of r-aminobutyric acid type A receptor subtypes by thalamic afferents in developing rat neocortex. Proc Natl Acad Sci USA 1997; 94: 6995–7000.
Pierson CR, Folkerth RD, Billiards SS, Trachtenberg FL, Drinkwater ME, Volpe JJ, et al. Gray matter injury associated with periventricular leukomalacia in the premature infant. Acta Neuropathol 2007; 114: 619–31.
Piñon MC, Jethwa A, Jacobs E, Campagnoni A, Molnár Z. Dynamic integration of subplate neurons into the cortical barrel field circuitry during postnatal development in the Golli-tau-eGFP (GTE) mouse. J Physiol 2009; 587: 1903–15.

Platt MJ, Cans C, Johnson A, Surman G, Topp M, Torrioli MG, et al. Trends in cerebral palsy among infants of very low birthweight (<1500 g) or born prematurely (<32 weeks) in 16 European centres: a database study. Lancet 369: 43–50.

Rezaie P, Dean A. Periventricular leukomalacia, inflammation and white matter lesions within the developing nervous system. Neuropathology 2002; 22: 106–32.

Robinson S, Li Q, Dechant A, Cohen ML. Neonatal loss of gamma-aminobutyric acid pathway expression after human perinatal brain injury. J Neurosurg 2006; 104 (6 Suppl): 396–408.

Schwartz-Bloom RD, Sah R. Gamma-Aminobutyric acid(A) neurotransmission and cerebral ischemia. J Neurochem 2001; 77: 353–71.

Skranes J, Vangberg TR, Kulseng S, Indredavik MS, Evensen KA, Martinussen M, et al. Clinical findings and white matter abnormalities seen on diffusion tensor imaging in adolescents with very low birth weight. Brain 2007; 130: 654–66.

Smith SM, Jenkison M, Johansen-Berg H, Rueckert D, Nichols TE, Mackay CE, et al. Tract-based spatial statistics: voxelwise analysis of multi-subject diffusion data. Neuroimage 2006; 31: 1487–505.

Smith SM, Nichols TE. Threshold-free cluster enhancement: addressing problems of smoothing, threshold dependence and localisation in cluster inference. Neuroimage 2009; 44: 83–98.

Stone BS, Zhang J, Mack DW, Mori S, Martin LJ, Northington FJ. Delayed neural network degeneration after neonatal hypoxia-ischemia. Ann Neurol 2008; 64: 535–46.

Tzourio-Mazoyer N, Landeau B, Papathanassiou D, Crivello F, Etard O, Delcroix N, et al. Automated anatomical labeling of activations in SPM using a macroscopic anatomical parcellation of the MNI MRI single-subject brain. Neuroimage 2002; 15: 273–89.

Vangberg TR, Skranes J, Dale AM, Martinussen M, Brubakk AM, Haraldseth O. Changes in white matter diffusion anisotropy in adolescents born prematurely. Neuroimage 2006; 32: 1538–48.

Volpe JJ. Brain injury in premature infants: a complex amalgam of destructive and developmental disturbances. Lancet Neurol 2009; 8: 110–24.

Weissenbacher A, Kasess C, Gerstl F, Lanzenberger R, Moser E, Windischberger C. Correlations and anticorrelations in resting-state functional connectivity MRI: a quantitative comparison of preprocessing strategies. Neuroimage 2009; 47: 1408–16.

Woodward LJ, Anderson PJ, Austin NC, Howard K, Inder TE. Neonatal MRI to predict neurodevelopmental outcomes in preterm infants. N Engl J Med 2006; 355: 685–94.

Wu YW, Escobar GJ, Grether JK, Croen LA, Greene JD, Newman TB. Chorioamnionitis and cerebral palsy in term and near-term infants. JAMA 2003; 290: 2677–84.

Yamauchi H, Kudoh T, Kishibe Y, Iwasaki J, Kagawa S. Selective neuronal damage and chronic hemodynamic cerebral ischemia. Ann Neurol 2007; 61: 454–65.